AIP | The Journal of Chemical Physics

State-resolved collisional energy transfer in highly excited NO 2 . I. Cross sections and propensities for J, K, and m J changing collisions

Bernd Abel, Norbert Lange, Florian Reiche, and Jürgen Troe

Citation: The Journal of Chemical Physics **110**, 1389 (1999); doi: 10.1063/1.478014
View online: http://dx.doi.org/10.1063/1.478014
View Table of Contents: http://scitation.aip.org/content/aip/journal/jcp/110/3?ver=pdfcov
Published by the AIP Publishing

State-resolved collisional energy transfer in highly excited NO_2. I. Cross sections and propensities for J, K, and m_J changing collisions

Bernd Abel,[a] Norbert Lange,[b] Florian Reiche, and Jürgen Troe
Institut für Physikalische, Chemie der Universität Göttingen, Tammannstrasse 6, D-37077 Göttingen, Germany

(Received 14 May 1998; accepted 5 October 1998)

State-resolved experiments probing the dynamics in $NO_2^{\#}$–NO_2 collisions at high internal energies ($17\,500 < E < 18\,000\ cm^{-1}$) are reported. A sequential optical double resonance technique with sensitive laser-induced fluorescence detection has been employed for the assignment of states of NO_2 in the energy range between 17 500 and 18 000 cm^{-1}, a spectral region where the optically ''bright'' $^2B_2$ state is strongly coupled to high lying (''dark'') states of the $^2A_1$ ground state and other electronic states. Subsequently, the decay of population and polarization following rotationally inelastic and elastic collisions has been probed directly using a time- and polarization-resolved optical double resonance technique. Total depopulation rates have been determined to be about 2–3 times above the Lennard-Jones estimate. The thermally averaged state-to-state cross sections have been derived from a master equation analysis of the kinetic traces. The rate constants have been scaled by angular momentum scaling expressions based upon the infinite order sudden approximation which were modified to account for dynamical restrictions on angular momentum and polarization transfer. Pure rotational energy transfer within a vibrational state turned out to be fast and dominating the collision dynamics, whereas rovibrational energy transfer was slower and proceeded with a lower efficiency. In addition, interesting propensity pattern for angular momentum and polarization transfer have been found. The individual state-to-state rate constants clearly indicated that rotational energy transfer in highly excited mixed (chaotic) states is still governed by pronounced propensities in J, K, and m_J changing collisions. Here m_j is the projection of J on a space fixed axis, which is defined by the laser, and K is the projection of J on the body-fixed symmetry axis of the molecule. In particular, we have found a propensity for small changes of m_J in elastic and inelastic collisions, in accord with recently suggested theoretical models. Interestingly, we also found a considerably lower probability for ΔK changes in these collisions. The propensities found for Δm_J and ΔK are discussed within the framework of dynamic (kinematic) collision models. The observed cross sections, their overall scaling behavior, as well as estimations of the Massey parameter are consistent with collisions following mostly a direct mechanism for rotational energy transfer rather than a complex forming mechanism.
[S0021-9606(99)00302-5]

I. INTRODUCTION

The determination of efficiencies and propensities for collision-induced inelastic processes in small molecules is of fundamental interest because these experiments provide a probe of the collision dynamics and the interaction potential, particularly its anisotropy.[1–8] An appealing aspect of state-resolved experiments at chemically significant energies is their ability to provide data that can be compared with theoretical calculations employing a relatively small amount of averaging; and that they may provide a realistic glimpse of the collision dynamics in situations where collisional energy transfer competes with reaction dynamics, a situation which is encountered in collisions of highly excited NO_2 colliding with (cold) NO_2. In spite of this fundamental interest, only a very limited number of direct, state-resolved experimental data on the relaxation of polyatomic molecules at high vibrational energy exist. This results mostly from experimental difficulties in the state-selective preparation and the detection of the energized molecules. However, recent laser based double resonance type experiments on C_2H_2,[9–13] HCN,[14] NO_2,[15] and H_2CO,[16–18] which directly monitored the energy and population redistribution within the highly excited polyatomic molecules, provided a first picture of collisional energy transfer at energies above 10 000 cm^{-1}. In contrast, at low internal energies, detailed studies are much more common, leading to a consistent physical picture of inelastic processes in this regime.[8,19–21] NO_2 has also been the subject of numerous non-state-resolved spectroscopy based energy transfer measurements at quite high internal energies for nearly 2 decades,[22–26] but in these experiments the resolution was not sufficient to separate rotational energy transfer from the overall relaxation of the molecule.

Theory and theoretical models for the treatment of ''slow'' collisions and ''fast'' collisions have been reviewed

[a]Electronic mail: BABEL@gwdg.de
[b]Present address: DGR-LPAS, Ecole Polytechnique Federale de Lausanne, 1015 Lausanne, Switzerland.

by many authors. Most of the rotational energy transfer experiments have been compared with theoretical models based upon (inpulsive) scattering theory,[27–32] often in the infinite order sudden approximation or based upon the Born approximation. Takayanagi,[33] Sakimoto,[34] Dashevskaya *et al.*,[35] Nikitin *et al.*,[36] and Nikitin and Umanskii,[37] on the other hand, have developed models which work particularly well for lower collision energies, and in cases where the energy transfer in collisions is dominated by nonadiabatic transitions between the various potential energy surfaces of the approaching species.

As far as state-resolved rotational energy transfer is concerned, there has been much recent interest in the determination of the extent to which the projection of the rotational angular momentum, J, on a space fixed axis, m_J, is conserved in elastic and inelastic collisions of small molecules in cell experiments. However, the extent to which the laboratory projection of J, m_J, is conserved for an asymmetric top in gas phase collisions has not been extensively studied. In a classical picture, reorientation results for a collider exerting a torque on a rotating molecule to turn it about an axis perpendicular to the rotational angular momentum vector. Changes in m_J in single-collision events may be classified as elastic or inelastic. Elastic reorientation (J reorientation) is any collisional event in which m_J is changed, but all other quantum numbers are unchanged. In inelastic collision events the rotational quantum numbers J and/or K are changed in addition to m_J. In either case the loss of orientation or alignment of a molecular ensemble is very important for the collision dynamics since these processes are dominated by the anisotropy of the weak, long-range interaction potential which tips the angular momentum vector J, relative to the space-fixed axis and is therefore of considerable interest since it is difficult to obtain information on this part of the potential energy surface. Therefore the data and conclusions from direct measurements of the polarization decay in NO_2–NO_2 collisions are of considerable stereodynamical significance and a challenge for theoretical models. Unfortunately, the experimental body of data in the literature from experiments with polarization resolution did not provide a consistent picture about the extent of which m_J is conserved in a collision. The experimental findings range from strict[38] m_J conservation to partial[39] m_J conservation and from a dipolar m_J, dependence with no single-collision elastic contribution[18] to significant elastic reorientation.[40] Recent reviews describe these experiments and their significance in terms of collision theories.[3,41] In parallel to this experimental work there have been considerable theoretical efforts in the calculation of fully m_J state-resolved inelastic cross sections for particular atom–molecule systems, and in the developments of models to explain the existence or absence of constraints on changes in m_J in inelastic and elastic collisions.[29,31,32,38,42–44]

Changes in K, the projection of the molecular angular momentum J on the molecule axis, have hardly been investigated. To our knowledge this is the first detailed investigation of propensities in ΔJ, Δm_J, and ΔK at the same time in a polyatomic molecule.

The outline of the present paper is as follows: First we will introduce the double resonance technique and the details of the experimental setup. We will in turn recall general theory to scale state-to-state rate constants in this type of experiment and introduce our model for the evaluation of the kinetic traces. Then, we will present the results and comprehensively discuss the observed propensities found for the change in angular momentum and its projections on a molecule and space fixed axis. Finally, we give a summary of the conclusions.

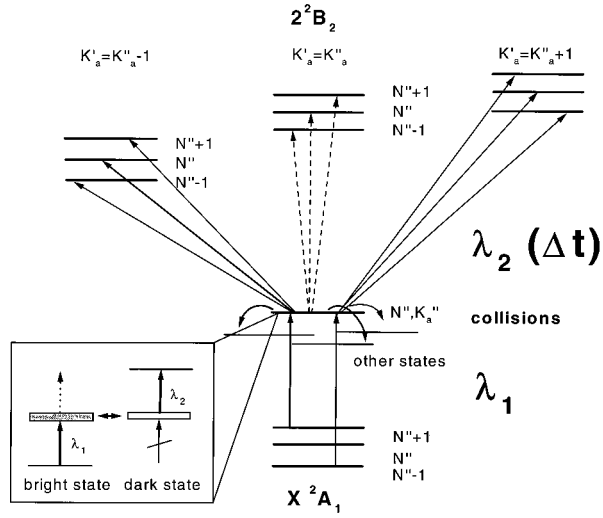

FIG. 1. Pump and probe excitation scheme. For a particular spectroscopic experiment λ_1 or λ_2 is fixed and the other is scanned. The resulting double resonance spectra provide unambiguous assignments for the intermediate state. In this particular energy region the intermediate state is heavily perturbed and coupled to dark states which provide most of the Franck–Condon intensity for the second step. The double resonance is monitored by observation of the excited state ($2\,^2B_2$) fluorescence. In a kinetic experiment λ_1 and λ_2 are fixed but the delay between the two is varied.

II. TECHNIQUE

The optical double resonance technique has been described in detail in Ref. 15, so only a brief description will be given here. According to Fig. 1 we first used the optical double resonance technique ($2\,^2B_2 \leftarrow {}''^2B_2/{}^2A_1'' \leftarrow {}^2A_1$) for the assignments of the NO_2 eigenstates. The stepwise excitation of the NO_2 followed by the observation of the ultraviolet (UV) emission corresponding to the $2\,^2B_2 \rightarrow X\,^2A_1$ transition provided simple double resonance spectra that could be easily assigned and analyzed by using the well-established molecular parameters of the initial $X\,^2A_1(0,0,0)$ and final $2\,^2B_2(0,0,0)$ states. Then, the time-resolved double resonance technique was employed for the energy transfer measurements. In this case the first laser pulse was used to prepare an initial rovibrational population, and the second laser probed the subsequent growth and decay of population, either in the initially prepared state or other states, populated by the specific energy transfer processes. The occurrence of the double resonance was monitored by observing the UV fluorescence corresponding to the radiative transition from the final state ($2\,^2B_2$) to the ground state ($X\,^2A_1$) Owing to the short lifetime of the molecules in the $2\,^2B_2$ state the fluorescence (yield) is not affected by collisions.[45] With the

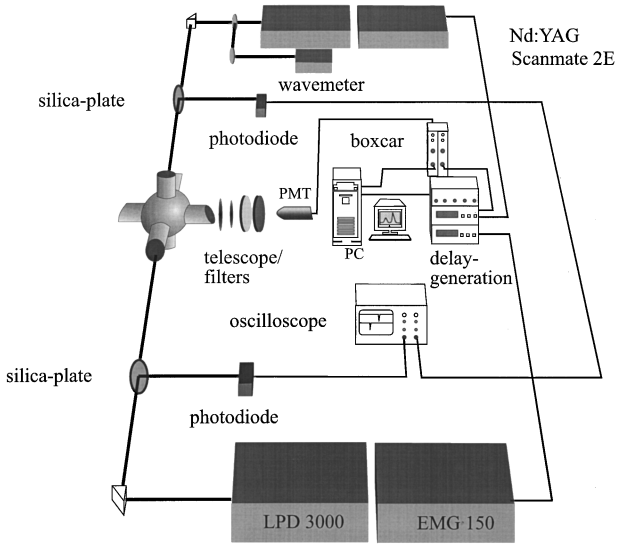

FIG. 2. Experimental setup for the spectroscopic and kinetic double resonance experiments.

known $^2A_1$ ground and $2\,^2B_2$ excited state spectroscopy[45,46] the ν_2 and the ν_1 scanned spectrum provided unambiguous assignments for the intermediate states. With a variable time delay between the two laser pulses of frequency ν_1 and ν_2 the growth and decay of population in initially prepared or neighboring states coupled to the first one by collisions could be monitored. The advantage over nontime-resolved techniques is that with a time-resolved technique we were able to distinguish single-collision effects from those arising from multiple collisions. The polarizations of the two lasers were set parallel or perpendicular to each other depending on the type of experiment.

III. EXPERIMENT

A diagram of the experimental apparatus is depicted in Fig. 2. The output of a dye laser (Lambda Physik Scanmate 2E, bandwidth: 0.03 cm^{-1}, pulse length: 10 ns) operated with an intracavity etalon and pumped by the second harmonic of a Continuum NY81C-10 was used to excite NO_2 and prepare high concentrations in specific excited eigenstates of the molecules. A XeCl excimer laser/dye laser combination (Lambda Physik EMG MSC/Lambda Physik LPD 3000) with pulse energies and widths of 10–15 mJ and 15 ns, respectively, with a bandwidth of 0.3 cm^{-1} or 0.04 cm^{-1} (etalon) was used to probe the initially populated levels or levels populated through collisions. The two laser beams were counterpropagated in a static stainless-steel cell that contained the sample of NO_2 molecules at pressures of 150–700 μbar. The $2\,^2B_2 \rightarrow X\,^2A_1$ fluorescence was collected perpendicular to the laser beams using an $f/1{:}2$ optics with two lenses, a pinhole, and a UV color filter (Schott UG11), and detected by a Thorn EMI 9635 QB photomultiplier. A Burleigh Instruments WA 5500 wavemeter was employed for the wavelength calibration and an SR DG535 delay generator together with two photodiodes and a LeCroy oscilloscope were used to set and control the time delay between the two pulses. The pressure of NO_2 was determined by a capacitance pressure gauge (Baratron). NO_2 was obtained from Messer–Griesheim (98%) and used without further purification.

IV. DOUBLE RESONANCE SPECTROSCOPY OF NO_2 EIGENSTATES

Direct measurements of the evolution of population of intermediate states are possible in this type of experiment by tuning the two lasers to the corresponding pump and probe transitions and changing the time delay between the pulses. In order to properly interpret time- and polarization-resolved optical double resonance experiments, it is necessary to have a spectroscopically well characterized and representative set of states. To obtain such a set of states and the best corresponding pump and probe transitions we use sequential double resonance spectroscopy, for the assignment and identification of molecular eigenstates, as described in Ref. 15. All states have been found to be strongly perturbed and mixed.[47,48] However, even in this case where vibronic chaos is established among the vibrational levels of highly excited states the eigenstates could in all cases be unambiguously assigned by this technique. Representative double resonance spectra for the intermediate states 30(1) and 90(1) (short notation for $N=3$, $K=0$, $J=3.5$, ν_1 and $N=9$, $K=0$, $J=3.5$, ν_1, see also Table I) are shown in Figs. 3 and 4. The relevant eigenstates for rovibrational energy transfer relevant to this investigation are tabulated in Table I. The spectral region of interest has been studied, assigned, and analyzed earlier by Shibuya *et al.*[49] and by the authors,[15] and for the spectroscopic peculiarities of this spectral region, and of the features of the highly mixed and perturbed eigenstates of NO_2, we refer to Refs. 15 and 49.

V. RADIATIVE LIFETIMES AND INTRAMOLECULAR DYNAMICS

The fluorescence lifetime of the NO_2 molecule is known to be longer than 5 μs in this energy region,[26,50] while the processes under investigation are much faster. To ensure that the observed changes of population in the intermediate states were caused only by energy transfer in collisions and not by radiative decay total depopulation rates of the states under investigation were measured at different pressures. The $p-\tau$ plot did not show any deviation from the expected pressure dependence and very little offset (probably due to beam fly-out) such that loss of population by fluorescence could be neglected safely under our conditions. It should be noted that all excited states under investigation are eigenstates of the NO_2 molecule, which means that they do not show any time dependent (intramolecular) dynamics themselves. This was tested in pump–probe experiments in a supersonic jet under experimental conditions where no collisions occur. Due to the fact that NO_2 is a stable radical the total angular momentum J of this molecule is half integral and defined by $J=N \pm S$. J can be assigned in almost all cases with our double resonance technique, although, it is generally difficult to fully resolve the spin splitting in high resolution absorption-like spectra. However, in the energy transfer experiments we make use of the approximation that we treat the molecule as

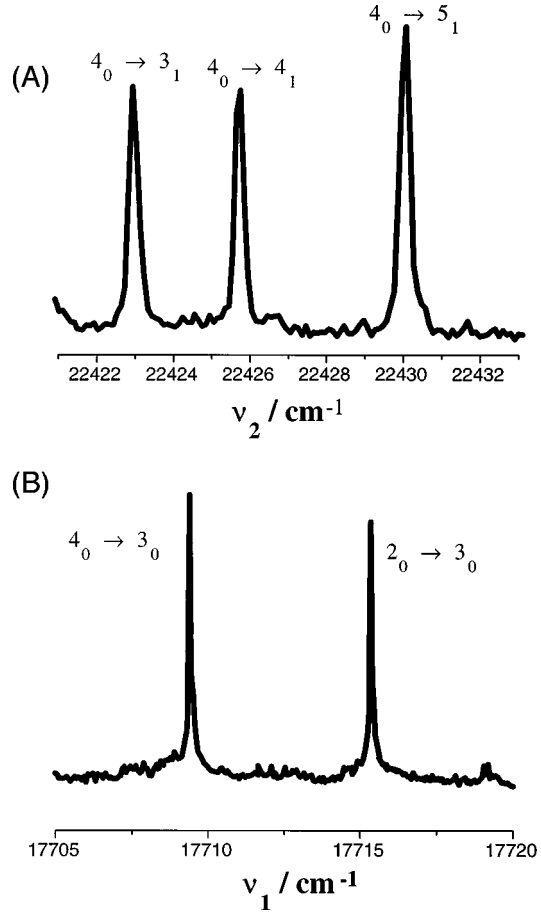

FIG. 3. Typical double resonance spectra for the assignment of an intermediate state at 17 716.33 cm^{-1}. (A) λ_1 fixed and λ_2 scanned and (B) λ_2 fixed and λ_1 scanned. In this particular case $N=3$, $K=0$, $J=3.5$.

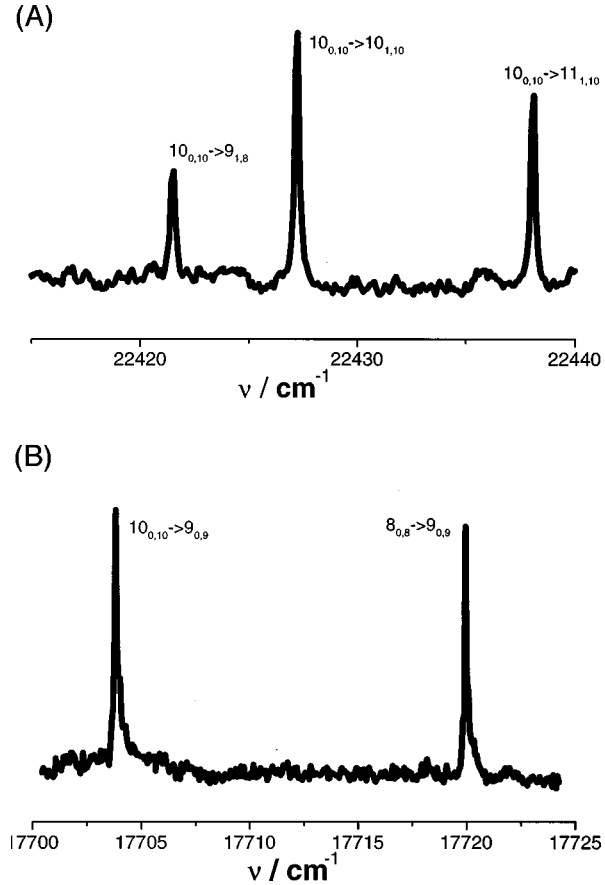

FIG. 4. Typical double resonance spectra for the assignment of an intermediate state at 17 750.07 cm^{-1}. (A) λ_1 fixed and λ_2 scanned and (B) λ_2 fixed and λ_1 scanned. In this particular case $N=9$, $K=0$, $J=9.5$.

a closed shell particle with an angular momentum quantum number N. We will come back to this approximation later (see also part II of this series) and discuss potential differences between open and closed shell particles and discuss the (possibly hidden) impact of ''open shells'' on the vibrational energy transfer of highly excited species. Although N is, in this case, not a rigorously conserved quantum number (only total angular momentum J is conserved) in all cases N could be assigned as well as J, and in modeling the energy transfer traces we found out that it is sufficient to consider the changes of K and angular momentum N (without spin) in the rotational energy transfer of the molecule. Therefore an angular momentum change of $\Delta J=n$ in all cases means that N changed by n. For the spectroscopy of these states we refer to Refs. 15 and 49.

TABLE I. OODR transitions[a] and assignments in the 563–566 nm range.

$N(\nu_{Pump})$	$K_a(\nu_{Pump})$	Vib. No.[b]	Energy/cm^{-1}	Pump trans.	ν_{Pump}/cm^{-1}	Probe trans.	ν_{probe}/cm^{-1}	label/ Ref.
3	0	1	17 716.33	$(3,0)' \leftarrow (4,0)''$	17 707.92	$(5,1) \leftarrow (''4,0'')'$	22 431.43	30(1)[c,d]
5	0	1	17 724.33	$(5,0)' \leftarrow (6,0)''$	17 706.60	$(7,1) \leftarrow (''6,0'')'$	22 434.04	50(1)[c,d]
7	0	1	17 736.08	$(7,0)' \leftarrow (8,0)''$	17 705.66	$(9,1) \leftarrow (''8,0'')'$	22 435.71	70(1)[c,d]
9	0	1	17 750.07	$(9,0)' \leftarrow (10,0)''$	17 703.83	$(11,1) \leftarrow (''10,0'')'$	22 437.92	90(1)[c,d]
8	1	1	17 751.06	$(8,1)' \leftarrow (7,1)''$	17 719.75	$(10,2) \leftarrow (''9,1'')'$	22 431.13	81(1)[c,d]
13	0	1	17 773.06	$(13,0)' \leftarrow (12,0)''$	17 707.27	$(11,1) \leftarrow (''12,0'')'$	22 408.4	130(1)[c,d]
6	1	1	17 737.92	$(6,1)' \leftarrow (5,1)''$	17 717.85	$(6,2) \leftarrow (''7,1'')'$	22 419.2	61(1)[c,d]
11	1	1	17 777.20	$(11,1)' \leftarrow (10,1)''$	17 722.56	$(11,0) \leftarrow (''12,1'')'$	22 399.2	111(1)[c,d]

[a]In general there are two transitions for the pump and 3–6 transitions (depending on K_a) for the probe laser (see double resonance spectra). We list here only the transitions which have been used in the energy transfer experiments and which are free from spectral overlap with other transitions. The wavelength calibration is accurate within 0.01–0.02 cm^{-1}. The primes ″, ′, and no prime denotes the ground state, intermediate state, and final excited state, respectively.
[b]Although the vibrational quantum numbers cannot be assigned in this energy region the rotational levels belonging to the same vibration can be found by plotting the term energies of the states vs. $J(J+1)$. J is in this case N (the rotational angular momentum without spin) and the spin S is not considered here.
[c]This work.
[d]Shibuya *et al.*, J. Phys. Chem. **97**, 8889 (1993).

VI. "SCALING" ROTATIONAL ENERGY TRANSFER CROSS SECTIONS

A general problem in state-resolved energy transfer experiments involving polyatomic molecules is the large number of levels involved and the large number of rate constants connecting these levels. However, it is generally recognized that the quantum state-resolved rate coefficients of the system are (in general) not completely independent such that they can be scaled by a fitting or scaling law expression. Scaling laws for inelastic processes and the differences between scaling and fitting laws have been reviewed by several authors.[3] The procedure for the evaluation of rotational energy transfer data from state, polarization, and time-resolved experiments is straightforward, and well known in principle, but may also be quite subtle.

In any case, we first have to answer the question how the individual state-to-state rate constants can be scaled in a model and what the correct physical picture is. Obviously, the collision energy, which is a function of relative velocity with respect to the rotational period, determines whether the collisions are close to the impulsive or sudden limit or are closer to the complex-forming limit. Rabitz *et al.*[28] and Alexander *et al.*,[27,31] as well as others have developed theoretical models based upon scattering theory in the sudden approximation which allow for a straightforward scaling of state-to-state rates. These scaling expressions may even be modified and corrected for a finite collision duration.[28] However, in the limit of slow collisions Nikitin and Umanskii,[37] Dashevskaya *et al.*,[35] Takayanagi,[33] and Sakimoto[34] developed theoretical models for slow complex forming (not direct impulsive) collisions. In these models changes in quantum numbers due to collisions are considered to be the result of distinct nonadiabatic transitions among the various potential energy surfaces of the approaching (and strongly interacting) molecules or radicals. Unfortunately, in this case simple scaling relations are much more difficult to obtain. We want to emphasize that the decision whether one or the other mechanism is dominant or whether both mechanisms compete cannot be answered *a priori*, because in many thermal experiments the collision energies are not so high that the sudden limit or the Born approximation will automatically be justified in any case. We have estimated the adiabaticity (Massey) factor ξ for the experimental conditions to be below 1 for almost all state-to-state cross sections, such that we believe that we are closer to the impulsive limit than to the complex-forming limit in our case and under our experimental conditions. We therefore used scaling expressions based upon the infinite order sudden approximation (IOSA) which turned out to be able to successfully and straightforwardly scale the state-to-state rates in our system. The justification for this approach will be given in Sec. VIII.

The scaling law for diatomics colliding with a structureless particle (atom) can be described (within the sudden approximation) by

$$k_{if}^{\mathrm{IOS}}=(2j_f+1)\exp\left(\frac{E_{j_i}-E_{j>}}{kT}\right)\times\sum_{\Lambda}\begin{pmatrix} j_i & j_f & \Lambda \\ 0 & 0 & 0\end{pmatrix}^2\cdot(2\Lambda+1)k_{\Lambda\to 0}, \tag{1}$$

with

$$k_{\Lambda\to 0}=A(T)\cdot[\Lambda(\Lambda+1)]^{-\alpha}. \tag{1a}$$

Here $j>$ denotes the level with the larger energy and the expression in brackets (:::) is a $3j$ symbol. The summation in Eq. (1) runs over all allowed rotational angular momentum changes Λ. In Eq. (1) detailed balance is automatically ensured by the factor in front of the summation. Equation (1) is valid for planar collisions only with the relative velocity vector in the plane of rotation. Therefore the corresponding values in the $3j$ symbol (lower row) are restricted to zero, accordingly. For polyatomic molecules (colliding with a polyatomic molecule) the basis rates $k_{\Lambda\to 0}$ can hardly be calculated from theory. Therefore, the parametrization of the basis rates is necessary, in general. Several approaches in this direction are described in the literature. The most popular model basis is given in Eq. (1a). This particular basis set (in the power basis) was first applied in combination with the IOS scaling law by Wainger *et al.*[51] to Na_2 collisions with polyatomic molecules (IOS-P). In order to account for the finite duration of a collision and possible additional restrictions in angular momentum transfer the energy corrected sudden scaling law (ECS-EP) has been proposed.[52]

$$k_{if}^{\mathrm{ECS-EP}}=(2j_f+1)\exp\left(\frac{E_{j_i}-E_{j>}}{kT}\right)\times\sum_{\Lambda}\begin{pmatrix} j_i & j_f & \Lambda \\ 0 & 0 & 0\end{pmatrix}^2 \cdot A(j_i,j_f,\Lambda)^2\cdot(2\Lambda+1)\cdot\exp[-\beta\cdot\Lambda(\Lambda+1)]\cdot k_{\Lambda\to 0}, \tag{2}$$

with $k_{\Lambda\to 0}=A(T)\cdot[\Lambda(\Lambda+1)]^{-\alpha}$. $A(j_1,j_2,\Lambda)$ is an adiabaticity correction which accounts for the finite duration of a collision. In some cases there are additional (dynamical) restrictions on the amount of angular momentum which can be transferred in a collision. This may be taken into account by modifying the basis rates with an exponential attenuation term $\exp[-\beta\Lambda(\Lambda+1)]$ [where $\beta^{-1}=j^*(j^*+1)$ and j^* is the orbital momentum of the system]. This modification has been shown to give an excellent representation of the experimental data. For $A(j_1,j_2,\Lambda)=1$ and $\beta=0$ one recovers the IOS scaling law.

Scaling laws for symmetric-top collisions (with structureless or structured particles) are different from those derived for diatomic molecules. This is mostly due to the fact that the molecule has two projections of J, namely m_J and K (the magnetic quantum number and K the quantum number, respectively). The eigenfunctions[29,53] in this case are

$$\varphi_{J,m_J,K}=\sqrt{[J]/8\pi^2}D^J_{K,m_J}, \tag{3}$$

with $[J]$ being the degeneracy of J and $D^J_{K,mJ}$ being the Wigner D functions.[1] In this case J is the rotor quantum number, m_J its projection on the space fixed z axis, and K its

projection on the body-fixed symmetry axis of the molecule. For a symmetric top-atom collision Rabitz *et al.*[29] give the coupling integral

$$\Theta(j,m_j,k,j',m_j',k',\Lambda,\Sigma,\Delta) = (-1^{k-m_j})\cdot\sqrt{[j][j'][j]}\cdot\begin{pmatrix} j & j' & \Lambda \\ -m & m' & \Sigma \end{pmatrix} \times\begin{pmatrix} j & j' & \Lambda \\ -k & k' & \Delta \end{pmatrix}, \tag{4}$$

where $[x]=2x+1$.

A general scaling expression within the energy corrected sudden (ECS) approximation for atom symmetric top collisions has been given by Rabitz:

$$k_{jmk\to j'm'k'}(T)=\sum_{\Lambda\Sigma\Delta}[\Theta(j,m_j,k,j',m_j',k',\Lambda,\Sigma,\Delta)]^2 \cdot A(\tau_c)\cdot k_{\Lambda\to 0}(T). \tag{5}$$

Provided Eq. (4) is valid, in the case of $K=0$ and $\Delta K=0$, the m_J dependence of rotationally inelastic collisions is given by[27]

$$k_{jm\to j'm'}(T)=(2j_i+1)\cdot(2j_f+1)\cdot\sum_{\Lambda\Sigma}(2\Lambda+1) \times\begin{pmatrix} j_i & j_f & \Lambda \\ -m & m' & -\Sigma \end{pmatrix}^2\begin{pmatrix} j_i & j_f & \Lambda \\ 0 & 0 & 0 \end{pmatrix}^2 \cdot A(\tau)^2\cdot k_{\Lambda\to 0}(T) \tag{6}$$

and for the degeneracy averaged integral inelastic state-to-state rates one recovers

$$k_{jk,j'k'}=(2j_f+1)\cdot\sum_{\Lambda\Delta}\begin{pmatrix} j_i & j_f & \Lambda \\ -k & k' & \Delta \end{pmatrix}^2 \cdot A(\tau)^2\cdot(2\Lambda+1)\cdot k_{\Lambda\to 0}. \tag{7}$$

VII. RET MODEL

Due to the importance of the theoretical model for the results in the paper we will briefly outline some well known theory and concepts used in this work to extract thermally averaged state-to-state rotational energy transfer (RET) cross sections for NO_2–NO_2 collisions from polarization- and time-resolved optical double resonance experiments. Although, the initial and final states are completely resolved in our experiments the complete state-to-state matrix **K** can be obtained only by modeling the population changes in the detected levels.

In order to keep the number of energy levels and the number of coupled differential equations as low as possible we used a truncated set of levels and grouped together level families into global baths with and without feedback (e.g., the $K=3$ stack and level with $N>13$). Owing to the m degeneracy of $2J+1$, the dimensionality of the coupled differential system has already become quite large even for low J and K levels. The simplified model used in the present case is depicted in Fig. 5. NO_2 is an asymmetric top molecule but is in a first approximation a prolate symmetric top. The level

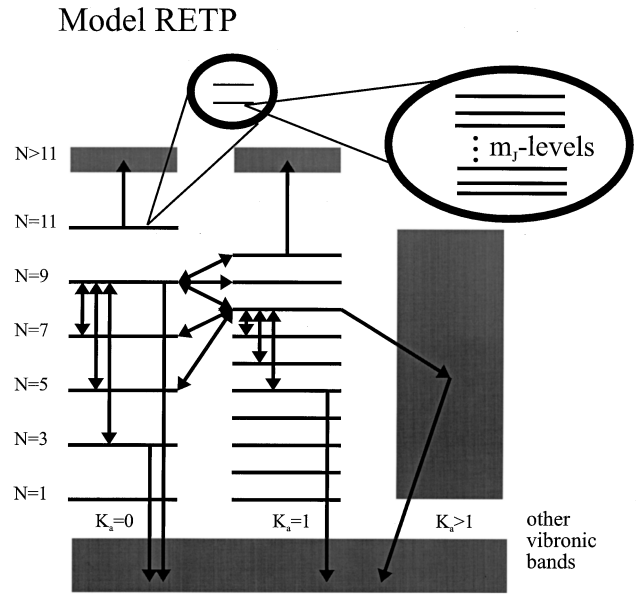

FIG. 5. The kinetic model for the determination of state-to-state cross sections from the linetic traces.

structure therefore resembles the typical K stack structure which is characteristic of prolate symmetric tops. For $K=0$ the nuclear spin statistics requires that rotational levels with even or odd values are missing, as well as one or the other level of the asymmetry doublets for $K\neq 0$, depending on the electronic state symmetry. In this particular case there are two vibrational states which are very close to each other, which had to be taken into account explicitly in the model (energy separation $\approx 1.2\ \mathrm{cm}^{-1}$).

The state-to-state thermally averaged cross sections are derived from a discrete master equation

$$\dot{P}=\mathbf{K}P, \tag{8}$$

with K being the rate coefficient matrix

$$K=\begin{pmatrix} k_{11} & \cdot & \cdot & k_{1j} \\ \cdot & \cdot & & \cdot \\ \cdot & & \cdot & \cdot \\ k_{i1} & \cdot & \cdot & k_{ij} \end{pmatrix} \tag{9}$$

for all rate constants connecting all considered levels. In our experiments we observe J, m_J, and K changing collisions. We therefore used a scaling law for nonelastic collisions that is able to scale ΔJ, Δm_J, and ΔK at the same time based upon Eq. (6) in the sudden limit $[A(\tau)=1]$ with the additional assumption that the collider (cold NO_2) behaves like a structureless particle (since we are not probing this particle and have no information about quantum changes either).

$$k_{jm\to j'm'}(T)=(2j_i+1)\cdot(2j_f+1)\cdot\sum_{\Lambda\Sigma}(2\Lambda+1) \times\begin{pmatrix} j & j' & \Lambda \\ -m & m' & -\Sigma \end{pmatrix}^2\begin{pmatrix} j_i & j_f & \Lambda \\ 0 & 0 & 0 \end{pmatrix}^2 \cdot F_K F_J(\Lambda)\cdot k_{\Lambda\to 0}(T) \tag{10}$$

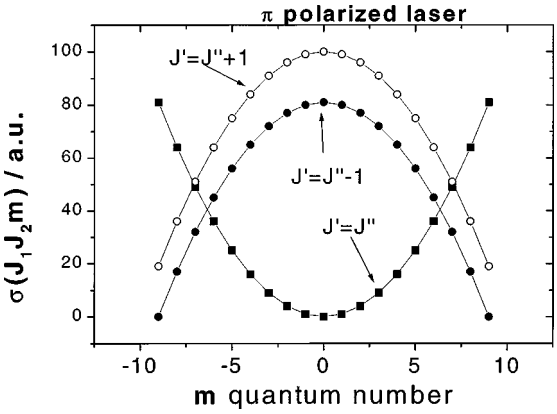

FIG. 6. Relative pump and probe cross sections for different m_J levels for linearly polarized lasers.

with $k_{\Lambda\to 0}(T)=a(T)\cdot[\Lambda(\Lambda+1)]^{-\alpha}$, $F_J(\Lambda)=\exp[-\beta\Lambda(\Lambda+1)]$ with $\beta^{-1}=j^*(j^*+1)$ (where j^* is the orbital momentum of the system), and $F_K=\exp(-\eta|\Delta K|)$.

In order to account for the additional restrictions on ΔK and Δm_J in angular momentum transfer we introduced, in addition, an exponential damping term for ΔJ and ΔK, as has been proposed for ΔJ in the ECS-EP in Eq. (2). As will be shown later the damping terms contain direct information about the dynamics of the collisions.

For the special case of elastic collisions, i.e., $\Delta m\neq 0$, $\Delta J=\Delta K=0$, we scaled the cross section according to

$$k_{jm\to j'm'}=\exp(-C|\Delta m|). \tag{11}$$

While these equations describe downward collisions the rates for upward transitions are determined by detailed balance.

According to Eq. (8) the time-dependent population vector $\mathbf{N}(t)$ could be calculated by integrating the set of coupled differential equations. To account for the time-dependent population of the pumped level by the pump source a time dependent source term was added to the corresponding equation:

$$\frac{dN_p}{dt}=\sum_j k_{pj}N_j+\alpha_L I(t), \tag{12}$$

where $I(t)$ is the experimental pulse profile of the pump laser and α_L is a phenomenological proportionality coefficient.

In order to model the time- (and polarization-) resolved traces and to calculate the (relative) m dependence of the cross sections $\sigma\ (J_1,J_2,m_J)$ has to be calculated for each individual pumped and probed Zeeman level. These cross sections can be expressed in terms of Clebsch–Gordan (or $3J$) coefficients and a reduced cross section $\sigma_{\rm av}(J_1,J_2)$ which is independent of m_J and describes the total intensity of the transition $J_1\to J_2$. The explicit evaluation[54] yields for a linearly polarized (π) laser beam (see Fig. 6):

$$\sigma_{\rm av}(J_1,J_2,m)=\begin{cases}\sigma_{\rm av}(J_1,J_2)\times[(J+1)^2-m^2] & \text{for } R \text{ lines}\\ \sigma_{\rm av}(J_1,J_2)\times m^2 & \text{for } Q \text{ lines}\\ \sigma_{\rm av}(J_1,J_2)\times(J^2-m^2) & \text{for } P \text{ lines.}\end{cases} \tag{13}$$

With these weight factors for different m_J levels (for pump and probe transitions) the time dependence of the polarization-resolved traces could be calculated.[54] The intensity was taken as a free parameter.

VIII. RESULTS AND DISCUSSION

In an ongoing study of collisional energy transfer of highly excited NO_2 we have found that the individual state-to-state rate constants and thermally averaged cross sections derived from a master equation analysis of the kinetic traces clearly indicate that rotational energy transfer in highly excited mixed (chaotic) states is still governed by pronounced propensities in J, K, and m_J changing collisions. Owing to the importance of J and K changing and the interest in m_j changing collisions in the study of dynamical stereochemistry we will entirely focus on rotationally inelastic and elastic collisions in the present paper and cover rovibrational energy transfer in the presence of strong chemical interaction in a proceeding paper (part II). Since we are mostly interested in the detailed dynamics of collisions in the presence of strong chemical interaction (where collision dynamics may compete with reaction dynamics $NO_2^{\#}+NO_2\Leftrightarrow O_2N-NO_2$) rather than collecting a large number of rate constants for many collision partners, we will focus here on collisions with only one collision partner, namely unexcited NO_2.

Note, the time axis throughout this work has been converted into a reduced axis $Z_{\rm LJ}[M]t$, which represents the number of Lennard-Jones collisions ($Z_{\rm LJ}=4.2\times10^{-10}\ {\rm cm^3\ s^{-1}}=13.4\ \mu{\rm s^{-1}\ Torr^{-1}}$). This reduced axis with $Z_{\rm LJ}$ as a reference (collision number) is very convenient since all experiments at different pressures can be processed simultaneously.

A. Total depopulation rates

The total depopulation rates of the different intermediate states were measured by pumping and probing the same intermediate level with parallel and perpendicular laser beams at variable time delay and monitoring the UV fluorescence from the final $2\ ^2B_2$ state. These measurements were carried out at different NO_2 pressures in the range of 150–500 μbar. Traces of typical total depopulation experiments for both relative polarizations are shown in Fig. 7. Pressure-independent total depopulation rates for parallel polarization were determined from $p-\tau$ plots fitting the decays as in Fig. 7 (upper trace) by a single exponential decay (zeroth order approximation). Total depopulation rates $k_{\rm td}$ determined this way in the considered energy range are between two and three times the Lennard-Jones estimate and a trend is observable that $k_{\rm td}$ increases slightly with increasing angular momentum J. Note, the fit in Fig. 7 does not represent a single exponential fit but a fit from the full kinetic model described above.

B. $k_{I\to J}(T)$ for J, K, and M_J changing NO_2–NO_2 collisions

In order to investigate rotational energy transfer in collisions between eigenstates with different J and K, we pumped one state of a specific vibrational level and probed a

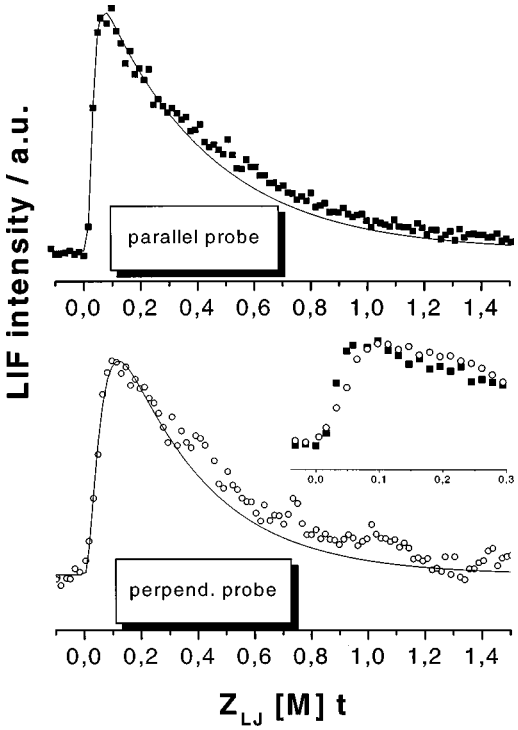

FIG. 7. Total depopulation traces for the 90(1) level for parallel (upper trace) and perpendicular (lower trace) polarizations of pump and probe beams (for the coding of levels see Table I). Bold squares and open circles: experiment; solid line: fit from the model. Note, the axis here has been converted into a reduced scale, i.e., in a scale displaying the number of Lennard-Jones collisions.

neighboring state close to the initial state but in the same vibrational state. Figures 8 and 9 show typical relaxation profiles. In the present paper we will examine only J, m_J, and K changing collisions with $\Delta K_a=0$ and $\Delta K_a=1$ with a focus on the m_J propensities but without vibrational energy transfer $(\Delta \nu_i=0)$. Quantitative estimates of individual state-to-state energy transfer rate constants and cross sections have been obtained by modeling the population changes in the detected levels by master equation simulation because in this type of experiment the observable double resonance signal contains contributions from all possible energy transfer pathways. With the above described model we have finally derived rate constants and thermally averaged cross sections for rotational and vibrational energy transfer by numerical integration of the set of differential equations and by modeling simultaneously all the kinetic traces obtained by state-resolved pump–probe spectroscopy. The final (best fit) results are shown in Tables II and III displayed in Figs. 8–13.

C. *J* changing collisions

The absolute rate constants as a function of the change in angular momentum $|\Delta J|$ are displayed in Figs. 10 and 11. It is obvious and expected that the cross sections strongly decrease with increasing angular momentum gap. However, large angular momentum changes in this collision system could still be observed easily, a point that will be discussed later. The parameters of the scaling expression [Eq. (10)] for the fit of the kinetic traces are given in Table II. The magnitude of the determined parameter α is close to the expected value.[52,55] As mentioned above the term $F_J(\Lambda)$ decreases the state-to-state cross sections further with respect to the original scaling expression given in Eq. (1). If we omitted this term in the scaling and fitting procedure the cross sections for higher $|\Delta J|$ were predicted to be significantly too high. We now turn to the significance and the role of the additional damping term $F_J(\Lambda)$ in Eq. (10). Following the discussion in Refs. 52 and 55 the change in angular momentum in a collision must come from the orbital angular momentum of the collision partners. In certain cases the amount of angular momentum which can be transferred in a collision is restricted, owing to an upper limit of the orbital angular momentum available in the collision. Brunner and Pritchard[55] pointed out that *one reason* for a breakdown of the power-law model may arise because of the the fact that real potentials have a repulsive core so that $V(R)$ will limit the distance of closest approach to some $R_m>0$. Since the anisotropy of the potential is finite at this point there must be a maximum l^* to the angular momentum which can be transferred in a collision. Classically $k_{l\to 0}$ will be zero for $l>l^*$ but quantum mechanically one might expect an exponentially decreasing $k_{l\to 0}$ reflecting the presence of tunneling.

This feature of the state-to-state rate constants may formally be taken care of by modifying the basis rates with an exponential attenuation term where $\beta^{-1}=j^*(j^*+1)$, and j^* is some upper limit on the number of angular momentum quanta which can be transferred in a collision. This means that j^* is a fit parameter, in principle, but its magnitude should be comparable with the orbital angular momentum available in the collision and can thus be estimated. With $\beta=2.4\times 10^{-2}$ we determined j^* to be 6.4 which is actually close to the estimated[52] average orbital angular momentum L_{av} for the collision partners at 300 K. Therefore, it is obvious that the damping term $F_J(\Lambda)$ is by no means arbitrary but can be predicted[52] from estimations of L_{av}, and is a direct consequence of the underlying collision dynamics. This also proves that the collisional energy transfer dynamics is governed by specific angular momentum transfer restrictions and propensities rather than by the corresponding energy gap, although angular momentum effects in collisions can be compensated partially by energy gap effects. If an energy gap scaling is used instead, an overall fit may be successful, but it will be difficult to correlate the energy-gap law parameters with the dynamics or physics of the collision process. The order of magnitude of cross sections for large angular momentum changes indicates that a simple dipole-like interaction and corresponding selection rules for the state-to-state cross sections is not sufficient. One may instead conclude that many terms of the multipole expansion of the intermolecular interaction can contribute; however, the dipole interaction term seems to make the largest contribution.

D. *K* changing collisions

In Table III and Fig. 11 the results for K changing collisions are given. The overall trend for the rates for J and K changing collisions with respect to J changing collisions with $\Delta K=0$ is that the latter are in general significantly larger. It appears to be a general feature in this collision system that changes in J are much more likely than changes

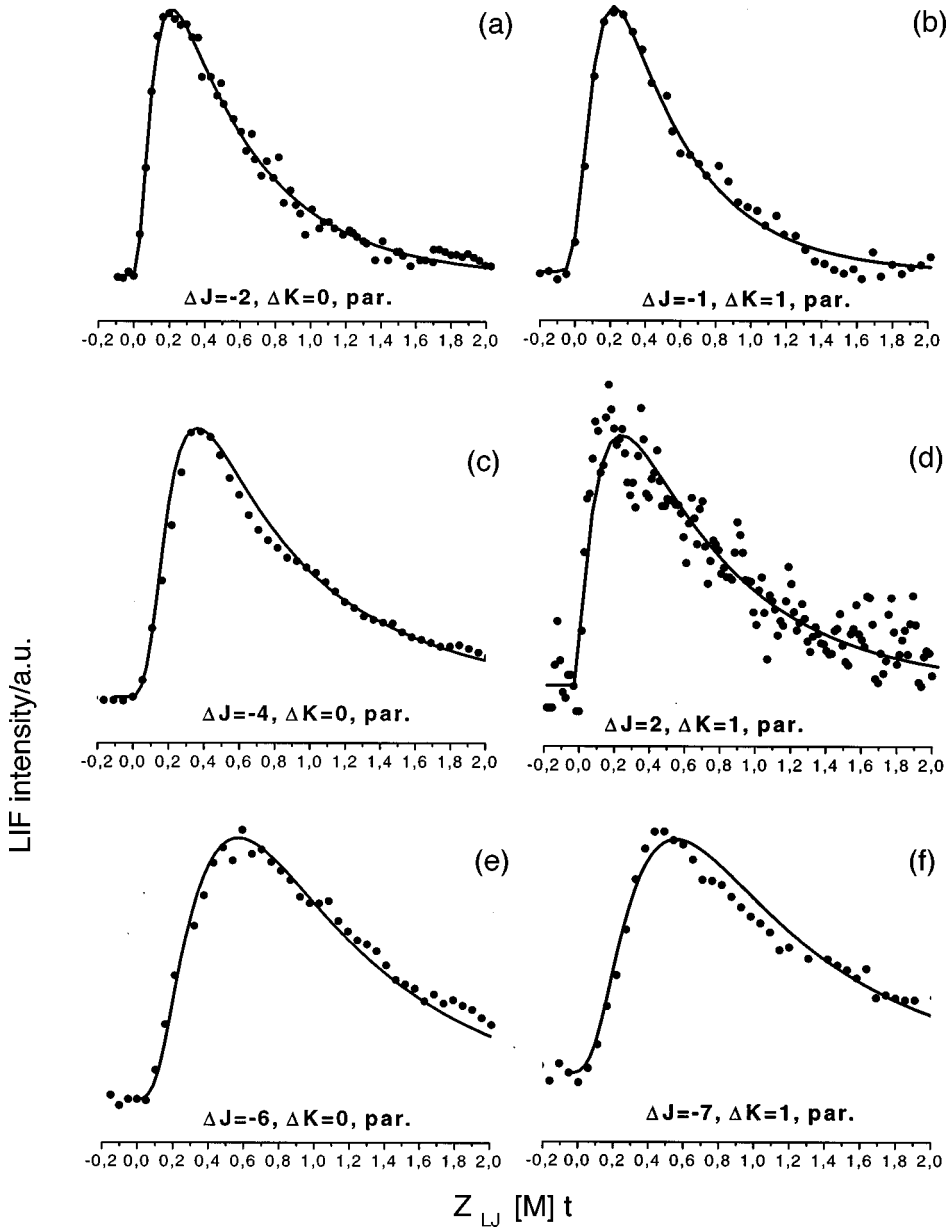

FIG. 8. Different kinetic traces and fits from the kinetic model. The initial state in traces (a)–(e) is 90(1) at 17 750.07 cm^{-1} (see Table I for the coding of states). The probed states are: (a) 70(1), (b) 81(1), (c) 50(1), (d) 111(1), (e) 30(1), and (f) pumped 130(1) at 17 737.92 cm^{-1} and probed 61(1).

in K or changes in both (with regard to the J changing collisions). The scaling expression for J and K changing collisions [Eq. (10)] included an attenuation (damping) term F_K which accounted for the K dependence of the observed cross section. Since the expression of Eq. (7) (i.e., the $3J$ symbol) shows a *too small* K dependence for the K changing state-to-state rates we used Eq. (10) instead, where the K dependence of the cross sections is solely made by the F_K term. In order to prove that this is more than just an additional term with an additional parameter η, which describes the angular momentum dependence of rotational cross sections, we have to discuss its significance and to show that this scaling law modification directly accounts for the special dynamical situation encountered here. While the first is easy to show because the quality of the fits for the kinetic traces was considerably poorer, the latter is slightly more complicated. In Fig. 14 we have illustrated a collision of a prolate symmetric top molecule with an atomic collider. Although, NO_2 is clearly an asymmetric top it may be approximated by a prolate symmetric top and the collision partner may be approximated as a structureless particle. As Oka[6] has already pointed out some time ago, in such a situation the excitation and deexcitation of the ''J rotor'' (in symmetric top notation) is much more likely than excitation of the ''K rotor'' because it is difficult for the collider to exert a large torque around the molecular axis. We would expect a different behavior for an oblate collider. This effect is interpreted as being due to the shape of the molecule; in a near prolate rotor like NO_2 the (short-range) interaction easily exerts a torque perpendicular to the molecular axis but cannot efficiently produce a torque around the molecular axis, thus changing the values of J with high probability, but without changing K easily. From this unexpected experimental observation we conclude that the lower probability for K changing collisions is a direct consequence of the kinematic collision dynamics. The parameter η can therefore be regarded as a correction of a zeroth-order scaling expression accounting for the shape of the molecule, other special constraints on ΔK, and other subtleties of the

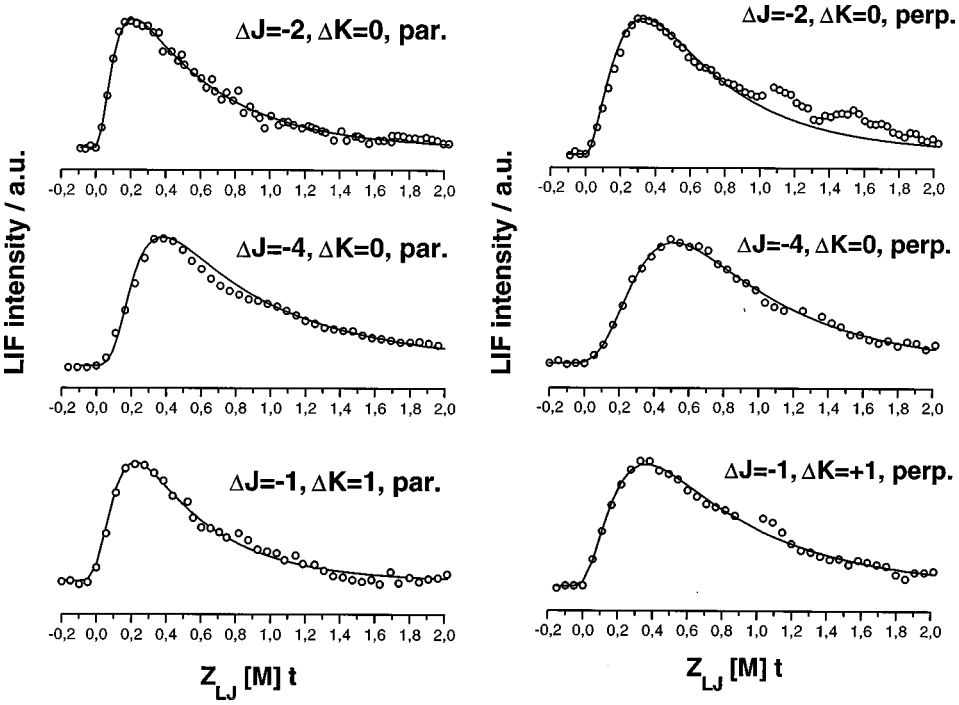

FIG. 9. Difference between parallel and perpendicular probe. Initial state is 90(1) at 17 750.07 cm^{-1} (see Table I for the coding of states). Probed states (from top to bottom) 70(1), 50(1), and 30(1).

collision dynamics in K changing collisions of a polyatomic molecule. Since most of the scaling expressions have been developed for diatomics our approach for a polyatomic molecule appears to be a straightforward extension. In order to compare our results with other experimental results without polarization dependence we also fitted the kinetic traces with an expression as Eq. (2) (with F_K included). The kinetic parameters given in Table II did not significantly reduce the quality of the fits compared to the full model with m_J resolution.

E. m_J changing collisions

We now turn to the m_J dependence of the cross sections obtained from polarization resolved pump–probe experiments. From a quantum treatment of rotationally inelastic collisions and a tensor expansion of the inelastic cross sections, Alexander and Davis[27] found for the integral cross sections of m_J resolved collision events:

$$\sigma_{JM\to J'M'}=\frac{\pi}{k_J^2}\sum_{KQ}\begin{pmatrix} J & J' & K \\ -M & M' & -Q \end{pmatrix}^2 P^K_{JJ'} \tag{14}$$

where k_J is the initial wave vector and P is the tensor opacity. If the collision time is shorter than the time which characterizes the dephasing of the initial and final rotational levels, then in the energy sudden limit the tensor opacity is given as[27]

$$P^K_{JJ'}=\frac{(2K+1)(2J+1)(2J'+1)k_J^2}{\pi}\begin{pmatrix} J & K & J' \\ 0 & 0 & 0 \end{pmatrix}^2 \sigma_{K\to 0}. \tag{15}$$

An insertion of Eq. (2) into Eq. (1) in turn gives

$$\sigma_{JM\to J'M'}=(2J+1)(2J'+1)\sum_{KQ}(2k+1) \times\begin{pmatrix} J & J' & K \\ -M & M' & -Q \end{pmatrix}^2\begin{pmatrix} J & J' & K \\ 0 & 0 & 0 \end{pmatrix}^2 \sigma_{K\to 0}. \tag{16}$$

Equation (15) (within the energy sudden limit) relates the m dependent cross sections for a particular $J\to J'$ transition to a vector of degeneracy averaged inelastic cross sections.

We have in turn used Alexander and Davis scaling expression for rotationally inelastic collisions and an exp $(-C|\Delta m_J|)$ expression for the scaling of elastic collision events which are probed to some extent by polarization-resolved three level total depopulation measurements. These results have been displayed in Figs. 12 and 13 and Table IV. It should be noted that the m_J dependence of the inelastic

TABLE II. Parameters for the kinetic RET model.

Parameters	Numerical value[a]	Dimension
m_J averaged (final state sum and initial state average).		
$J,K\to J',K'$		
a(T)	$9(\pm 1)\times 10^{-10}$	$cm^3\,s^{-1}$
α	$1(\pm 0.1)$	—
β	$2.4(\pm 0.3)\times 10^{-2}$	—
η	$1.5(\pm 0.2)$	—
m_J resolved:		
$J,K,m_j\to J',K',m_j$ with ΔJ and/or $\Delta K\neq 0$		
a(T)	$3.3(\pm 1)\times 10^{-11}$	$cm^3\,s^{-1}$
α	$1(\pm 0.1)$	—
β	$2.4(\pm 0.3)\times 10^{-2}$	—
η	$1.5(\pm 0.2)$	—
$J,K,m_j\to J',K',m_j$ with ΔJ and $\Delta K=0$ and $\Delta m_j\neq 0$		
$k=k_0\cdot\exp(-C\cdot\lvert\Delta m_j\rvert)$		
k_0	$1.9(\pm 0.5)\times 10^{-9}$	$cm^3\,s^{-1}$
C	$0.85(\pm 0.3)$	—

[a]k_σ ($cm^3\,s^{-1}$) is given here; to obtain the cross sections σ (Å^2), multiply by 1.912×10^{11}; to obtain k_Γ ($\mu s^{-1}\,Torr^{-1}$), multiply by 3.2624×10^{10}.

TABLE III. Direct state-to-state rate coefficients and cross sections from the kinetic RET model: m_J averaged (final state sum and initial state average): $J,K \rightarrow J',K'$.

$J_i=9,K_i=0\rightarrow J_f,K_f$	ΔJ	ΔK	k_σ (cm^3 s^{-1})	k_Γ (μs^{-1} Torr^{-1})	σ (Å^2)	Observed (+) predicted (0)
9,0→7,0	−2	0	2.5×10^{-10}	8.2	47.8	+
9,0→5,0	−4	0	6.7×10^{-11}	2.2	12.8	+
9,0→3,0	−6	0	1.8×10^{-11}	0.59	3.4	+
9,0→1,0	−8	0	2.5×10^{-12}	0.082	0.48	0
9,0→11,0	2	0	2.9×10^{-10}	9.5	55.4	0
9,0→13,0	4	0	8.1×10^{-11}	2.6	15.5	+
9,0→8,1	−1	1	1.2×10^{-10}	3.9	22.9	+
9,0→7,1	−2	1	5.1×10^{-11}	1.7	9.8	0
9,0→6,1	−3	1	2.6×10^{-11}	0.85	5.0	0
9,0→5,1	−4	1	1.3×10^{-11}	0.4	2.5	0
9,0→4,1	−5	1	6.6×10^{-12}	0.22	1.3	0
9,0→3,1	−6	1	3.1×10^{-12}	0.1	0.59	0
9,0→2,1	−7	1	1.4×10^{-12}	0.046	0.27	0
9,0→1,1	−8	1	5.1×10^{-13}	0.017	0.1	0
9,0→10,1	+1	1	1.2×10^{-10}	3.9	22.9	0
9,0→11,1	+2	1	5.5×10^{-11}	1.8	10.5	+
9,0→12,1	+3	1	2.9×10^{-11}	0.95	5.5	0
9,0→13,1	+4	1	1.6×10^{-11}	0.52	3.1	+

[a]k_σ (cm^3 s^{-1}) multiplied by 1.912×10^{11} yields σ (Å^2).
[b]k_σ (cm^3 s^{-1}) multiplied by 3.2624×10^{10} yields k_Γ (μs^{-1} Torr^{-1}).

collisions is solely given by the $3j$ symbol in Eq. (10), and that the m_J dependence of the pure elastic collisions is introduced by an additional exponential factor. A fit of an exponential decay to the rate constants for the inelastic m_J changing collisions as a function of $|\Delta m|$ gave the same exponential factor as the scaling law for the purely elastic rates. This means that the m_J dependence for the elastic and inelastic case appears to be the same within the experimental accuracy.

We now want to compare our results with the results from other experiments with polarization resolution. Some years ago, McCaffery,[3,38,41,56] Pritchard and co-workers[57] reported a series of experiments in which polarized laser induced fluorescence (PLIF) of laser excited *diatomic molecules* (I_2, Li_2, Na_2) has been measured. The principal conclusion from their investigations was that all data were consistent with the assumption of rigorous conservation of m_J, the projection of J onto a space fixed axis (laboratory fixed coordinate system). In particular, reorientation of the J vector with respect to a space fixed axis by elastic collisions was found to have low probabilities with cross sections typically two orders of magnitude lower than for J changing collisions. On the other hand the reanalyzed Na_2^*–Xe data of Pritchard[57] by de Pristo *et al.*[28] and the BaO RET experiments of Field *et al.*,[39] showed that for these diatomics m_J was neither conserved nor totally randomized in a laboratory frame in RET experiments.

The extent to which the laboratory projection m_J of the

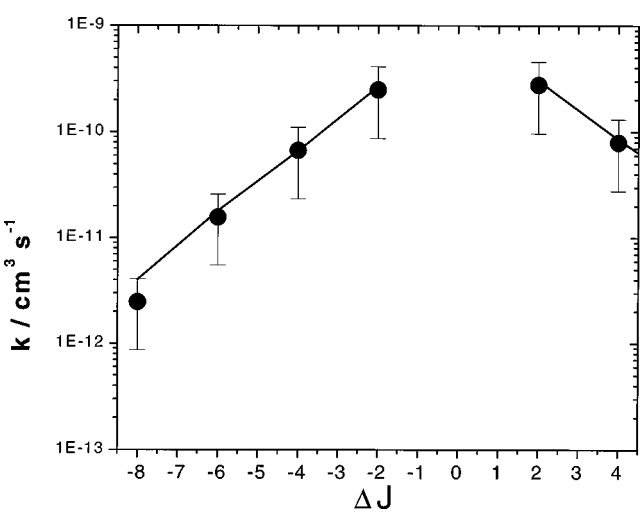

FIG. 10. m_J averaged state-to-state rate constants (propensities) for J changing collisions (leaving K unchanged) as a function of ΔJ. Filled dots: experiment; bold line: m_J averaged Eq. (10). Small deviations from the scaling law are due to final adjustments of the cross sections to improve the fit.

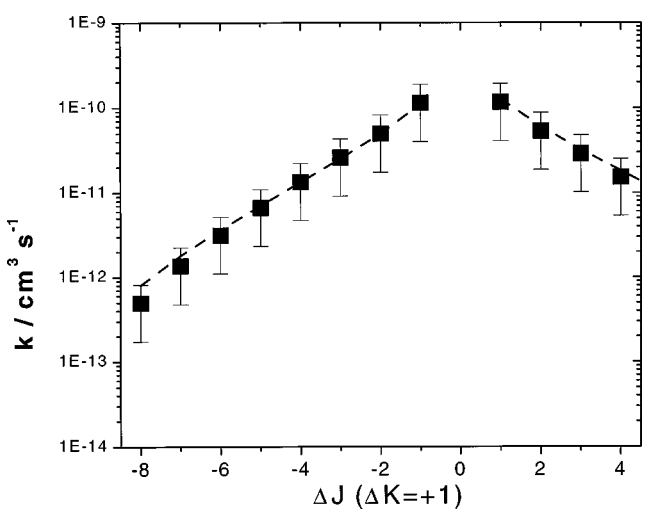

FIG. 11. m_J averaged state-to-state rate constants (propensities) for J and K changing ($\Delta K\pm1$) collisions as a function of ΔJ. Filled dots: experiment; dashed line: m_J averaged Eq. (10). Small deviations from the scaling law are due to small final adjustments of the cross sections to improve the fit.

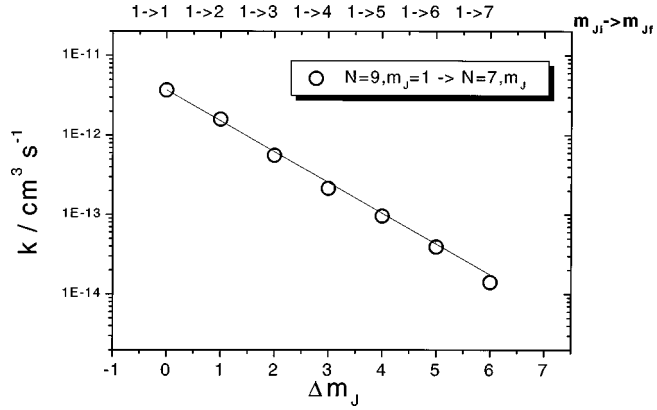

FIG. 12. State-to-state rate constants for m changing inelastic collisions as a function of Δm_J. In this particular case the initial state is 90(1) and the final state is 70(1). Open circles: experiment; solid line: a fit of an exponential decay to the rate constants for the inelastic m_J changing collisions as a function of $|\Delta m|$ gave the same exponential factor as the scaling law for the purely elastic rates (within the experimental accuracy).

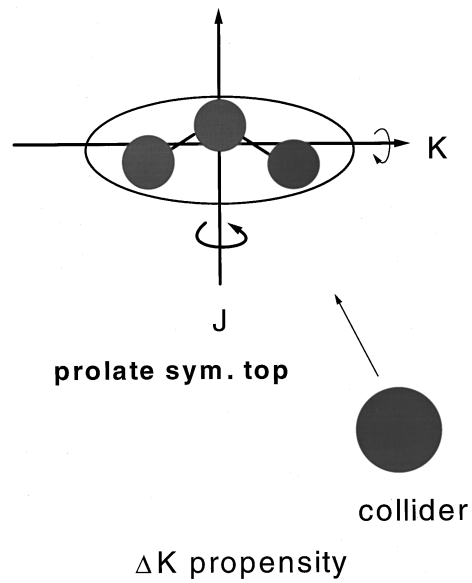

FIG. 14. Cartoon displaying a ΔK propensity due to the steric properties of the near prolate symmetric top, i.e., highly excited NO_2.

rotational angular momentum J is conserved for *polyatomic* molecules such as asymmetric or symmetric tops in gas phase collisions has received much less attention in the past. Wilson *et al.*[58] were among the first to examine the m_J dependence of RET in an asymmetric top, ethylene oxide, by microwave double resonance studies. They found that inelastic $\Delta m_J = 1$ processes accounted for most of the depolarization process. Recently, Vaccaro *et al.*[16] and Coy and co-workers[18] have published nice experimental results on the RET of formaldehyde (H_2CO) in the $^1A_2$ ($\nu_4 = 1$) state. Their principal findings from a detailed kinetic model were that there are no detectable contributions from elastic m_J changing collisions and that m_J is only changed by ± 1 in rotationally inelastic collisions consistent with the selection rules for a dipole–dipole interaction and anticipated from a leading dipolar term in the interaction potential of the collision partners. In contrast to these results, John *et al.*[40] determined the extent of collision induced J realignment in ground state H_2CO to be considerable. They found a large propensity for collisional relaxation to proceed via elastic realignment processes. In addition, they observed for many individual state-to-state transitions that large steps in m_J can occur. Very recently, Klaassen *et al.*[19] found that elastic reorientation collisions are significant in methane self-collisions and that they play a role in the polarization-resolved overall relaxation of this spherical top molecule. Recently, McCaffery and collaborators[59] have also investigated the polarized fluorescence of NH_2 in collisions where they again stress the importance of a selection rule $\Delta m_J = 0$ in rotationally elastic collisions. Results on m_J changing collisions in rotationally inelastic collisions in progress have not been published yet.

Our data do not confirm a total conservation of m_J, e.g., a propensity of $\Delta m_J = 0$, nor can we confirm that m_J is totally scrambled (statistical limit), but the data do show that for the asymmetric rotor NO_2, the quantum number m_J was neither conserved nor totally randomized in a laboratory frame after collisions leading to rotational energy transfer, in good agreement with theory.[27] Moreover, the m_J conservation we find as well as the scaling of inelastic state-to-state rate constants as a function of Δm_J follows closely the predictions from Alexander and Davis. In addition, we find a considerable fraction of elastic collisions which do change

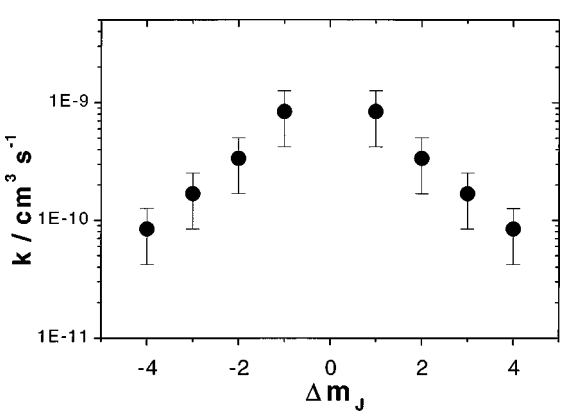

FIG. 13. State-to-state rate constants for m_J changing elastic collisions as a function of Δm_J that leave all other quantum numbers unchanged.

TABLE IV. Direct elastic m_J changing state-to-state rate coefficients and cross sections from the kinetic RET model: m_J resolved $J,K,m_j \rightarrow J'=J$, $K'=K$, $m_j' \neq m_j$ $(J=9, K=0)$.

Δm_J	k_σ (10^{-10} cm^3 s^{-1})	k_Γ (μs^{-1} Torr^{-1})[a]	σ (Å^2)[b]
−1	8.4	27.4	161
−2	3.4	11.1	65
−3	1.6	5.2	31
−4	0.8	2.6	15.3
1	8.4	27.4	161
2	3.4	11.1	65
3	1.7	5.2	31
4	0.8	2.6	15.3

[a] k_σ (cm^3 s^{-1}) multiplied by 1.912×10^{11} yields σ (Å^2).
[b] k_σ (cm^3 s^{-1}) multiplied by 3.2624×10^{10} yields k_Γ (μs^{-1} Torr^{-1}).

m_J but leave all other quantum numbers unchanged. With regard to the m_J conservation in elastic collisions NO_2 seems to behave differently than H_2CO.[18] The impact and importance of elastic reorientation contributions for the linewidths of molecular transitions has been discussed (see, e.g., Ref. 19 and references therein).

Regarding the origin of the Δm_J propensity and the collision mechanism, Alexander and co-workers have concluded that strict m_J conservation (propagated by many authors) may be only a sufficient rather than a necessary condition for agreement with the body of experimental data. They find that partial m_J conservation is a natural consequence of the nature or the mechanism of impulsive collisions, and derive scaling expressions in the energy sudden limit which we found to be able to scale our cross sections successfully without further assumptions. We also find a similar dependence of the elastic cross sections as a function of Δm_J for elastic collisions. It should be noted that Eq. (16) contains some important implications for the development of models for m_J conservation in rotationally inelastic collisions. As Alexander and Davis pointed out, a necessary condition for the validity of a strict $\Delta m_J = 0$ selection rule is the disappearance of the $3j$ symbol for $Q \neq 0$. This is clearly not the case such that it is difficult to explain a rigorous conservation of m in thermal cell experiments on the basis of Eq. (16). Finally, Alexander *et al.* found from a statistical analysis of experimental data that Θ conservation, where $\Theta = \cos^{-1}(Jz)$, the angle between the space fixed axis and the angular momentum vector J, is a more appropriate dynamical model than m_J conservation. These findings support a very simple picture for the conservation of m_J or the tilting angle Θ (with respect to the space fixed z axis) in molecular collisions. The colliding NO_2 molecule in such a case appears to resemble a spinning top (Fig. 15) with a propensity towards conserving the angular momentum and in turn the ''orientation'' of its rotational axis (in space) in an impulsive collision.

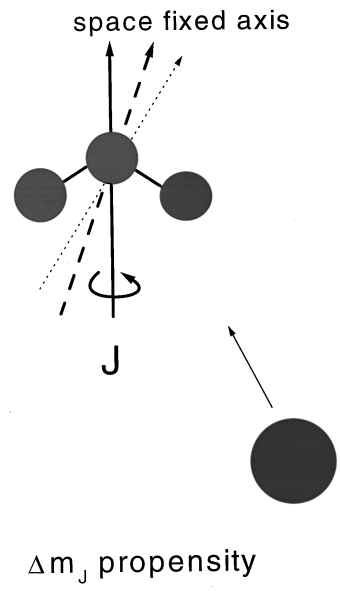

FIG. 15. Δm_J propensity in the kinematics in a collision of a spinning near prolate symmetric top, i.e., highly excited NO_2 and a structureless particle.

F. Complex-forming versus direct collisions

The experimental results from this work provide firm evidence for the conclusion that the collision mechanism for the collisions we observe in the experiments is closer to an impulsive collision rather than a complex forming collision. Note, we use the term complex forming (maybe in a different fashion than others) for collisions which lead to a long lived collision complex which exchanges energy (strong coupling) and which can be regarded as a recombination of the two particles leading to an energized ''supermolecule that in turn redissociates.'' The m_J conservation and the order of magnitude of the thermally averaged cross sections for the collisions (see also part II of this series), the adiabaticity parameter ξ (which is estimated to be always well below 1), as well as the overall scaling behavior point towards the conclusion that the kinematics rather than the association dynamics with nonadiabatic transitions is important in NO_2 self-collisions. This does not imply that other collisions do not occur, but our experiment appears to be not very sensitive to these collisions because they are expected to have a low probability. We have also neglected the adiabaticity correction in the scaling expressions which accounts for the finite duration of a collision. We have found that adiabaticity correction in the scaling expressions was not necessary, e.g., it did not improve the fits significantly, so we omitted this correction in order to reduce the number of free parameters in our fit. At the same time this confirms that the sudden approximation seems to be a reasonable approximation to derive the scaling expressions for our experimental situation. In general, the adiabaticity factors (multiplicative factors) may provide a reasonable correction for the finite duration of a collision, but it is meaningful only for small correction factors because for larger (significant) corrections one may encounter a situation where the (''kinematic'') approach is not justified anymore and the theoretical approach for ''slow collisions'' of Nikitin *et al.*,[37] Dashevskaya *et al.*,[35] Takayanagi,[33] and Sakimoto[34] has to be used.

G. Polarization moments and density matrix formalism

The overall relaxation in a multistate system is given by

$$\dot{n}_{\alpha jm} = \sum K_{ajm;\alpha' j' m'} n_{\alpha jm}, \tag{17}$$

where K contains all state-to-state (m resolved) relaxation rates, and α includes all quantum numbers other than J and m. In this case all relaxation processes are coupled. A simplification (decoupling) of Eq. (17) can be achieved from a linear transformation[60]

$$n'_{\alpha j \kappa} = \sum_m C^{JJ'}_{\kappa m} n_{\alpha jm}, \tag{18}$$

where the C coefficients are eigenvectors of the relaxation matrix K and are expressed by $3j$ symbols. The transformed Eq. (17) has the form

$$\dot{n}'_{\alpha j\kappa}=\sum_{J} K_{\kappa}^{JJ'} n'_{\alpha j\kappa}. \tag{19}$$

In this case the rate coefficients $K_K^{jj'}$ of the *state moments* or polarization moments $n'_{j\kappa}$ are independent, relax independently, and can be fitted independently.

Instead of populations n one may also involve the density matrix formalism[3]

$$\dot{\rho}=K\rho \tag{20}$$

and carry out a multipole expansion of the density matrix

$$^{jj'}\rho_Q^{\kappa}=\sum_{mm'} (-1)^{j-m}(2\kappa+1)^{1/2}\begin{pmatrix} j & j' & \kappa \\ m & -m & -Q \end{pmatrix}^{jj'} \rho_{mm'}, \tag{21}$$

where κ is the rank and defines the state multipole. If the space fixed z axis is chosen as the symmetry axis, only the $Q=0$ components in Eq. (21) survive, and the density matrix becomes diagonal and thus the state moments can be related to the occupation numbers of individual m levels. In optical absorption and emission, only the multipoles $\kappa=0,1,2$ are present and thus the series may be truncated at $\kappa=2$. In general, the names population, orientation, and alignment are used for $\kappa=0,1$, and 2. Under isotropic conditions, e.g., an experiment in a thermal cell, each multipole polarization is decoupled from all other multipole polarizations and decays with its own characteristic decay time.

The rate constants given in this work are those of the initial K matrix given in Eq. (16). They can, in principle, be transformed into independent relaxation rates of the state moments. It is not the purpose of the present article[61] to compare the different formalisms nor to transform the present data but to extract state specific rate constants and to investigate cross sections and the mechanisms of rotational energy and polarization transfer. In any case the different approaches are equivalent.

IX. SUMMARY AND CONCLUSIONS

In our recent work the NO_2 molecule has proven to be an excellent model system for quantum state-resolved investigations of collisional relaxation in small molecules at chemically significant internal energies in the presence of strong chemical interaction (leading to N_2O_4). The presented experiments are a demonstration of the power of time-resolved double resonance techniques in collisional energy transfer studies. It has been shown that state-to-state relaxation at very high vibrational energies can be resolved and understood in small molecules, even in the case of very strong excited state mixing, due to the power of time-resolved double resonance techniques. The principal findings from the present investigation are:

(a) Pure rotational energy transfer within a vibrational state turned out to be fast and to dominate the collision dynamics, whereas rovibrational energy transfer was slower and proceeded with a lower but still high efficiency.

(b) The individual state-to-state rate constants clearly indicated that rotational energy transfer in highly excited mixed (chaotic) states is still governed by pronounced propensities in ΔJ, ΔK, and Δm_J. In particular, we have found a propensity for small changes of m_J in elastic and inelastic collisions, in accord with recently suggested theoretical models and a smaller propensity to change the K quantum number in J and K changing collisions. These propensities can be understood within the framework of dynamic (kinematic) collision models.

(c) The observed cross sections, their overall scaling behavior, the polarization decay, as well as estimations of the Massey parameter ζ are consistent with collisions following mostly a direct mechanism for rotational energy transfer rather than a complex forming mechanism. The fact that complex forming collisions do not appear to play a role in the rotational energy transfer at high internal energies is striking since the well depth (the binding energy) between two NO_2 molecules is about 20 kT.

The information on the rotational energy transfer of a highly excited small molecule can be used to derive scaling expressions for the rotational energy transfer in two-dimensional master equations[4] describing the relaxation of highly excited small molecules in kinetic systems, and for the quantitative evaluation of line broadening in optical transitions of small molecules.

ACKNOWLEDGMENTS

Many stimulating discussions on special topics of this work with E. Nikitin, J. Steinfeld, B. Orr, and S. Coy, and financial support from the Deutsche Forschungsgemeinschaft (SFB 357 ''Molekulare Mechanismen Unimolekularer Prozesse,'' AB63/2-1/2) are gratefully acknowledged. The authors thank Steve Coy for the MATLAB and FORTRAN routines for some of the 3J symbol calculations. F.R. thanks the Fond der Chemischen Industrie and the BMFT for a graduate student fellowship.

[1] *Atom-Molecule Collision Theorie: A Guide for the Experimentalist*, edited by R. B. Bernstein (Plenum, New York, 1979).
[2] J. T. Yardley, *Introduction to Molecular Energy Transfer* (Academic, New York, 1980).
[3] A. J. McCaffery, M. J. Proctor, and B. J. Whitaker, Annu. Rev. Phys. Chem. **37**, 223 (1986).
[4] H. Hippler and J. Troe, in *Bimolecular Collisions (Advances in Gas-Phase Photochemistry and Kinetics)*, edited by M. N. R. Ashfold and J. E. Baggott (The Royal Society of Chemistry, London, 1989).
[5] R. E. Weston and G. W. Flynn, Annu. Rev. Phys. Chem. **43**, 559 (1992).
[6] T. Oka, in *Advances in Atomic and Molecular Physics*, edited by D. R. Bates and I. Easterman (Academic, New York, 1973), Vol. 9, p. 127.
[7] E. E. Nikitin, in *Physical Chemistry: An Advanced Treatise*, edited by H. Eyring, D. Henderson, and W. Jost (Academic, New York, 1974), Vol. 6A.
[8] B. J. Orr, *Advances in Chemical Kinetics and Dynamics* (JAI, New York, 1995), Vol. 2A, p. 21.
[9] A. P. Milce, H.-D. Barth, and B. J. Orr, J. Chem. Phys. **100**, 2398 (1994).
[10] A. P. Milce and B. J. Orr, J. Chem. Phys. **104**, 6423 (1996).
[11] J. D. Tobiason, M. D. Fritz, and F. F. Crim, J. Chem. Phys. **101**, 9642 (1994).
[12] A. P. Milce and B. J. Orr, J. Chem. Phys. (to be published).

[13] M. A. Payne, A. P. Milce, M. J. Frost, and B. J. Orr, Chem. Phys. Lett. (to be published).
[14] J. Wu, R. Huang, M. Gong, A. Saury, and E. Carrasquillo M., J. Chem. Phys. **99**, 6474 (1993).
[15] B. Abel, H. H. Hamann, and N. Lange, Faraday Discuss. **102**, 147 (1995).
[16] P. H. Vaccaro, F. Temps, S. Halle, R. W. Field, and J. L. Kinsey, J. Chem. Phys. **87**, 1895 (1988).
[17] F. Temps, S. Halle, P. H. Vaccaro, R. W. Field, and J. L. Kinsey, J. Chem. Soc., Faraday Trans. 2 **84**, 1457 (1988).
[18] S. L. Coy, S. D. Halle, J. L. Kinsey, and R. W. Field, J. Mol. Spectrosc. **153**, 340 (1992).
[19] J. J. Klaassen, S. L. Coy, J. I. Steinfeld, and B. Abel, J. Chem. Phys. **101**, 10533 (1994).
[20] B. Abel, S. L. Coy, J. J. Klaassen, and J. I. Steinfeld, J. Chem. Phys. **96**, 8236 (1992).
[21] R. Dopheide, W. Cronrath, and H. Zacharias, J. Chem. Phys. **101**, 5804 (1994).
[22] T. L. Mazely, R. R. Friedl, and S. P. Sander, J. Chem. Phys. **100**, 8040 (1994).
[23] J. J. F. McAndrew, J. M. Preses, R. E. Weston, and G. W. Flynn, J. Chem. Phys. **90**, 4772 (1989).
[24] S. M. Alder-Golden, J. Phys. Chem. **93**, 691 (1989).
[25] B. M. Toselli, T. L. Walunas, and J. R. Barker, J. Chem. Phys. **92**, 4793 (1990).
[26] S. M. Alder-Golden, J. Phys. Chem. **93**, 684 (1989).
[27] M. H. Alexander and S. L. Davis, J. Chem. Phys. **78**, 6754 (1983).
[28] R. Ramaswamy, A. E. DePristo, and H. Rabitz, Chem. Phys. Lett. **61**, 495 (1979).
[29] A. E. DePristo, S. D. Augustin, R. Ramaswamy, and H. Rabitz, J. Chem. Phys. **71**, 850 (1979).
[30] G. C. Corey and M. H. Alexander, J. Chem. Phys. **88**, 6931 (1988); **85**, 1859 (1986).
[31] S. L. Davis and M. H. Alexander, J. Chem. Phys. **78**, 800 (1983).
[32] M. H. Alexander and P. J. Dagdigian, J. Chem. Phys. **66**, 4126 (1977).
[33] K. Takayanagi, J. Phys. Soc. Jpn. **45**, 976 (1978).
[34] K. Sakimoto, J. Phys. Soc. Jpn. **48**, 1683 (1980).
[35] E. I. Dashevskaya, E. E. Nikitin, and J. Troe, J. Chem. Phys. **97**, 3318 (1992).
[36] E. E. Nikitin, J. Troe, and V. G. Ushakov, J. Phys. Chem. **98**, 3257 (1994).
[37] E. E. Nikitin and S. Ya. Umanskii, *Theory of Slow Atomic Collisions*, Springer Series in Chemical Physics, Vol. 30 (Springer, New York, 1984).
[38] H. Kato, S. R. Jeyes, A. J. McCaffery, and M. D. Rowe, Chem. Phys. Lett. **39**, 573 (1976).
[39] S. L. Silvers, R. A. Gottscho, and R. W. Field, J. Chem. Phys. **74**, 6000 (1981).
[40] J. W. C. Johns, A. R. W. McKellar, T. Oka, and M. Röhmheld, J. Chem. Phys. **62**, 1488 (1975).
[41] S. R. Jeyes, A. J. McCaffery, and M. D. Rowe, Mol. Phys. **36**, 1865 (1978).
[42] M. Elbel, Z. Phys. A **305**, 25 (1982).
[43] L. Monchick, J. Chem. Phys. **75**, 3377 (1981).
[44] Ph. Brechignac, A. Picard-Bersellini, R. Charneau, and J. M. Launay, Chem. Phys. **53**, 165 (1980).
[45] K. E. Hallin and A. J. Merer, Can. J. Phys. **54**, 1157 (1976).
[46] W. C. Bowman and F. C. De Lucia, J. Chem. Phys. **77**, 92 (1982).
[47] A. Delon, R. Jost, and M. Lombardi, J. Chem. Phys. **95**, 5701 (1991).
[48] J. L. Hardwick, J. Mol. Spectrosc. **85**, 109 (1985).
[49] K. Aoki, H. Nagai, K. Hoshina, and K. Shibuya, J. Phys. Chem. **97**, 8889 (1993).
[50] D. K. Hsu, D. L. Monts, and R. N. Zare, Spectral Atlas of Nitrogen Dioxde 553 to 648 nm (Academic, New York, 1978).
[51] M. Wainger, I. Al-Agil, T. A. Buner, A. W. Korp, N. Smith, and D. E. Pritchard, J. Chem. Phys. **71**, 1977 (1979).
[52] J. I. Steinfeld, P. Ruttenberg, G. Millot, G. Fanjoux, and B. Lavorel, J. Phys. Chem. **95**, 9638 (1991).
[53] D. A. Varshalovich, A. N. Moskalev, and V. K. Khersonskii, *Quantum Theory of Angular Momentum* (World Scientific, Singapore, 1988).
[54] R. N. Zare, *Angular Momentum, Understanding Spatial Aspects in Chemistry and Physics* (Wiley, New York, 1988).
[55] T. A. Brunner and D. Pritchard, in *Dynamics of the Excited State*, edited by K. P. Lawley (Wiley, New York, 1992).
[56] M. D. Rowe and A. J. McCaffery, Chem. Phys. **43**, 35 (1979).
[57] T. A. Brunner, R. D. Driver, N. Smith, and D. E. Pritchard, J. Chem. Phys. **70**, 4155 (1979).
[58] J. B. Cohen and E. B. Wilson, J. Chem. Phys. **58**, 456 (1973).
[59] K. Truhins, Z. T. Al Wahabi, M. Auzinsh, A. J. McCaffery, and Z. Rawi, J. Chem. Phys. **106**, 3477 (1997).
[60] E. Nikitin (private communication).
[61] B. Abel and F. Reiche, J. Chem. Phys. (to be published).